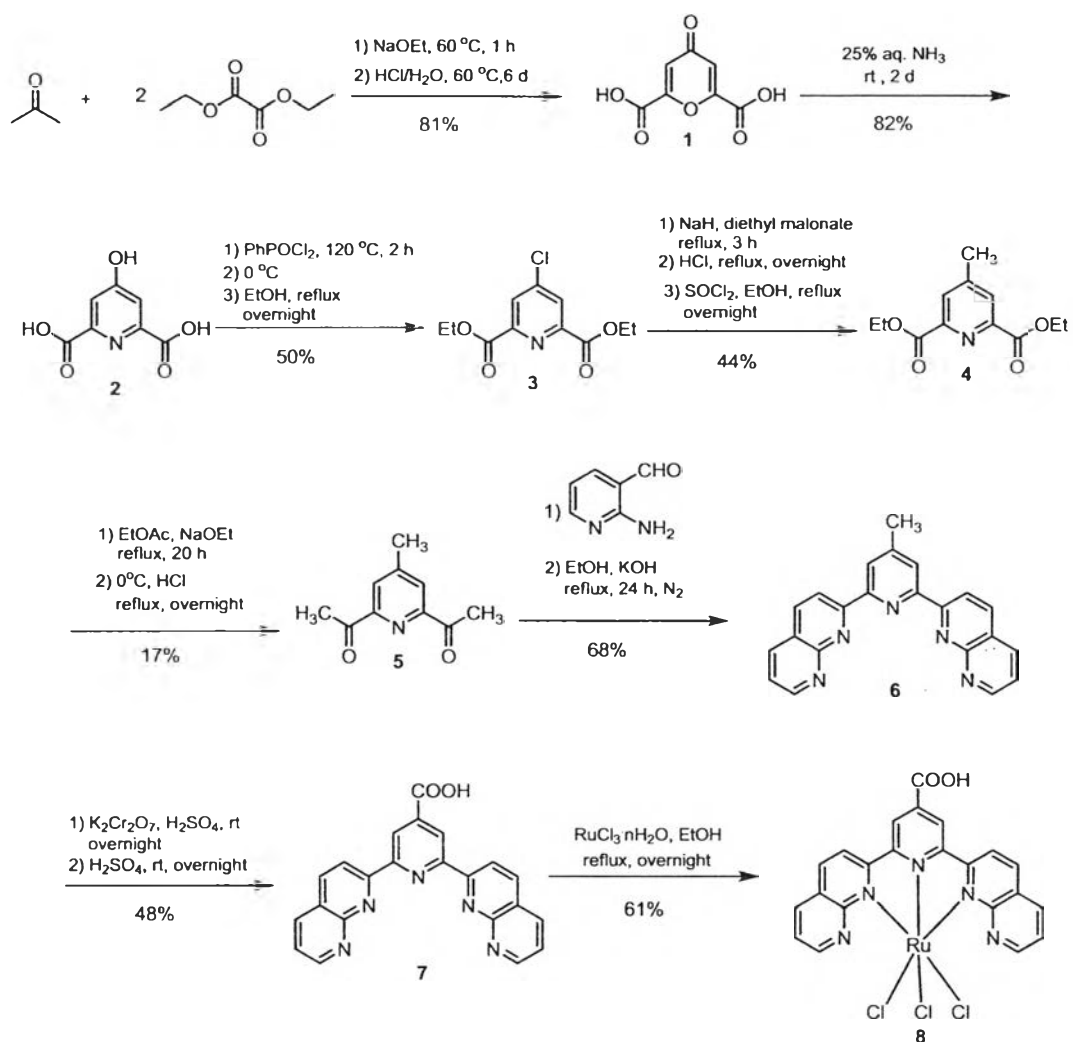


CHAPTER IV

RESULTS AND DISCUSSION

This research aimed to synthesis a bis-naphthyridyl pyridine derivative as an alternative photosensitizer for optoelectronic devices. Synthesis pathway for the target molecules 7 and 8 are shown in Scheme 4.1.

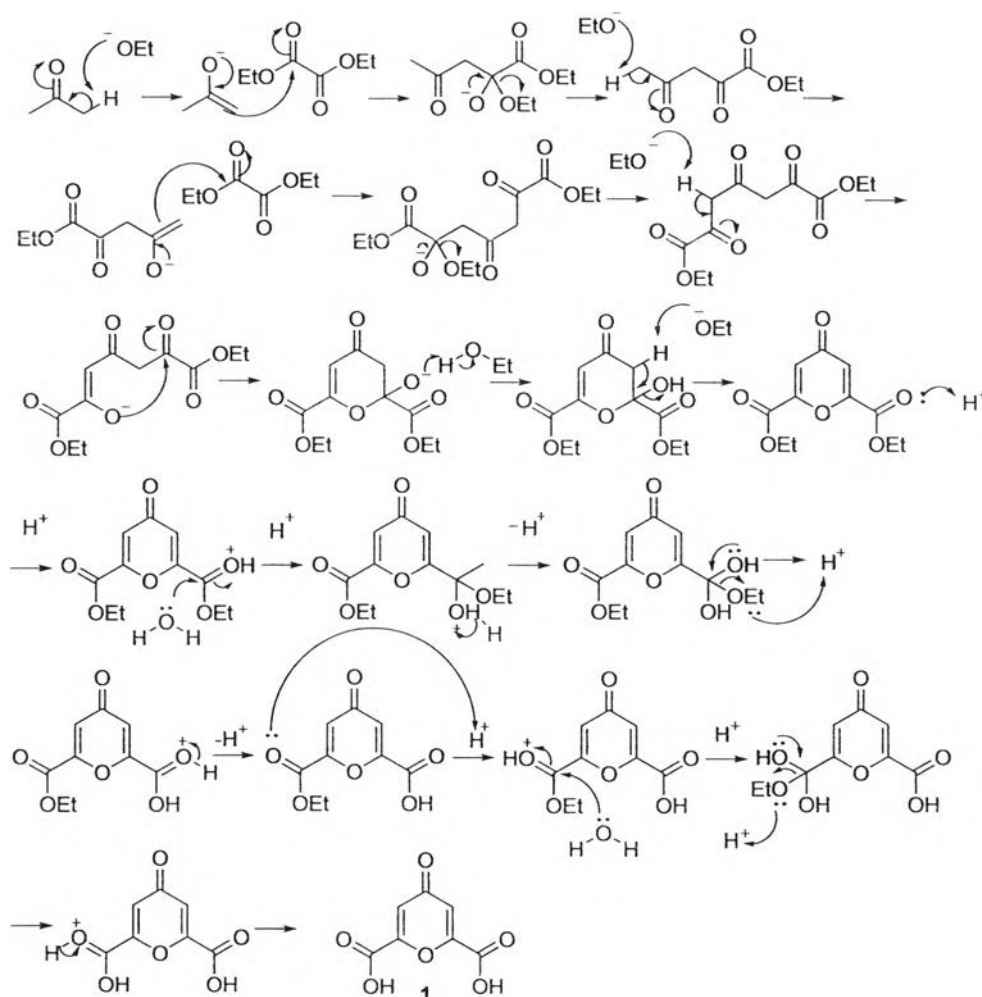


Scheme 4.1 Synthesis pathway of target compounds 7 and 8

4.1 Synthesis

4.1.1 Oxo-4H-pyran-2,6-dicarboxylic acid (1)

Compound 1 was successfully synthesized by aldol condensation between acetone and 2 equivalents of diethyl oxalate and subsequently *in situ* hydrolysis of the diester produced [29]. Mechanism for synthesis compound 1 is shown in Scheme 4.2.

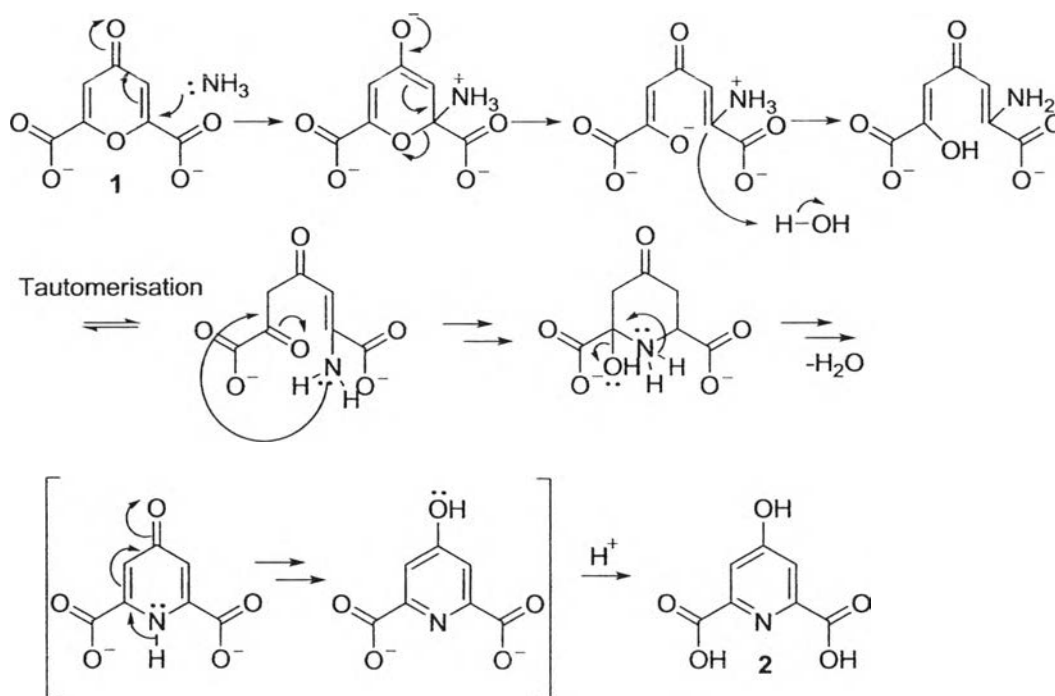


Scheme 4.2 Mechanism of the synthesis of compound 1

The $^1\text{H-NMR}$ spectrum of compound **1** showed a singlet signal of aromatic hydrogen protons at 6.86 ppm. (Figure A.1), confirming the formation of compound **1**.

4.1.2 Oxo-1,4-dihydropyridine-2,6-dicarboxylic acid (Chelidamic acid) (**2**)

Compound **2** was prepared from imination of compound **1** with ammonia solution [29]. Ammonia acted as a nucleophile attacking the carbon atom in position 2. Then the nitrogen atom coupled with carbonyl group to form the pyridine ring. Mechanism for synthesis compound **2** is shown in Scheme 4.3.

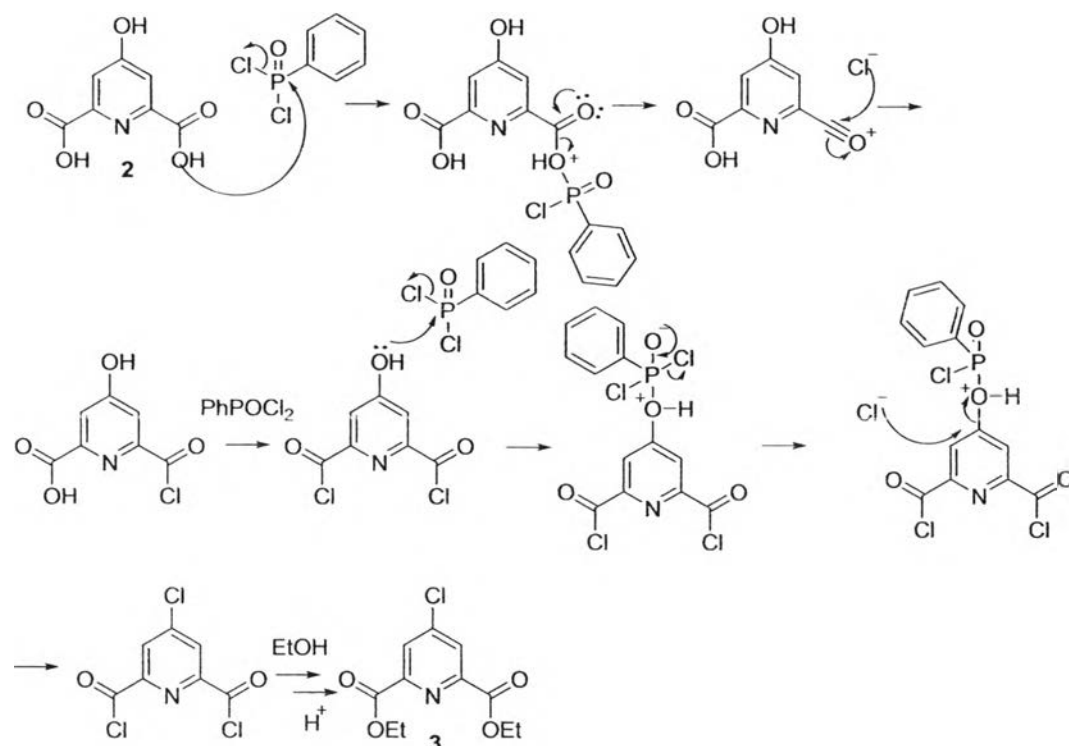


Scheme 4.3 Mechanism of the synthesis of compound **2**

The $^1\text{H-NMR}$ spectrum of compound **2** showed a singlet signal of pyridinyl protons at 7.56 ppm (Figure A.3) and the disappearance of the aromatic signal of compound **1** at 6.86 ppm, consistent with the results reported in the literature.

4.1.3 Diethyl 4-chloropyridine-2,6-dicarboxylate (3)

Compound 3 was successfully synthesized by chlorination of compound 2 with phenylphosphonic dichloride and esterification [30]. Mechanism for the synthesis of compound 3 is shown in Scheme 4.4.



Scheme 4.4 Mechanism of the synthesis of compound 3

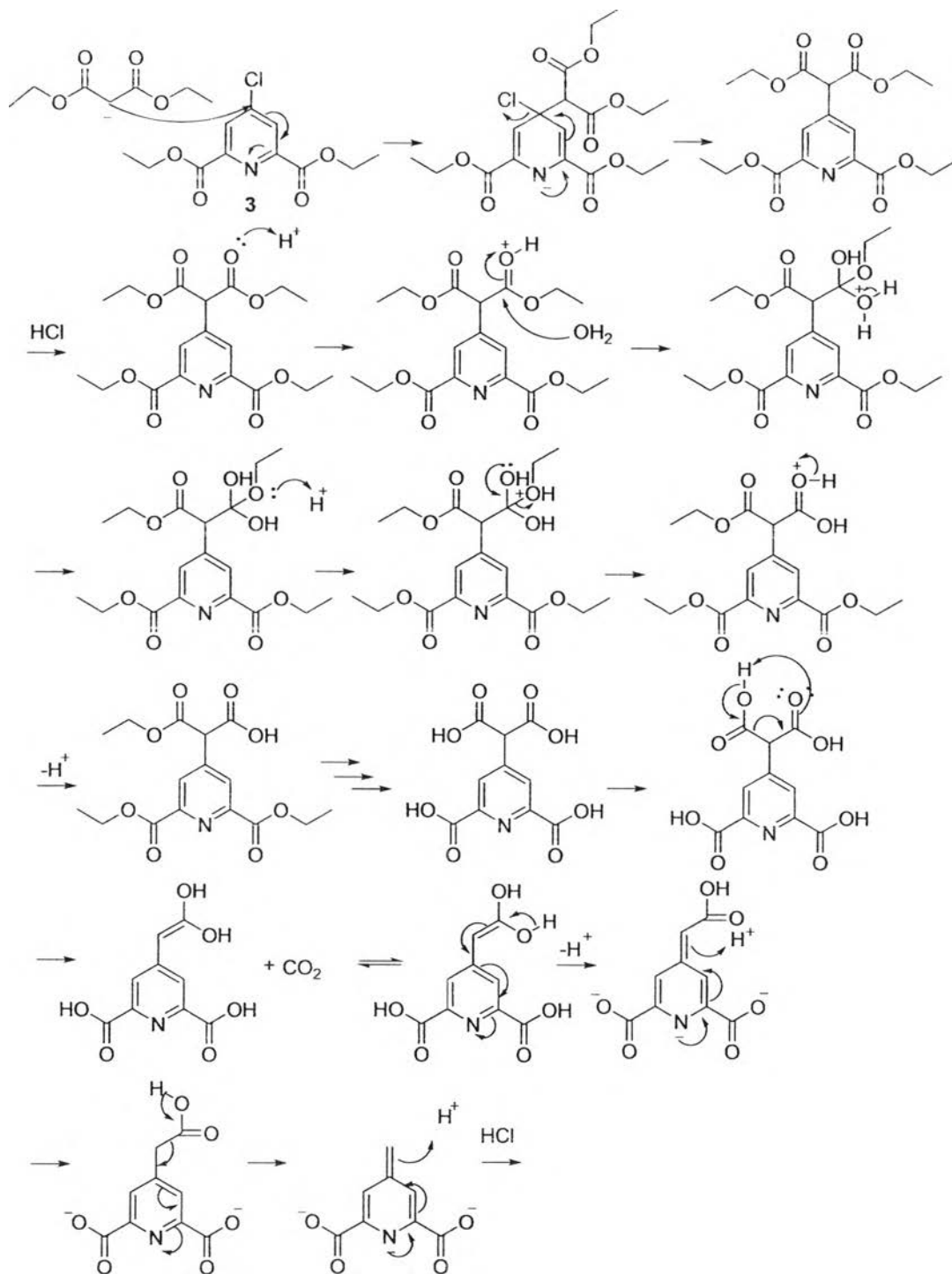
The ¹H-NMR spectrum of compound 3 showed a singlet signal of pyridinyl proton at 8.27 ppm (2H) which shifted to down field comparably with a singlet signal of pyridinyl proton of the compound 2 due to inductive effect of chloro group and the ethyl ester protons showed a quartet signal at 4.50 ppm (4H) coupling with a triplet signal at 1.46 ppm (6H) with coupling constants 7.2 Hz (Figure A.5), confirming the formation of compound 3.

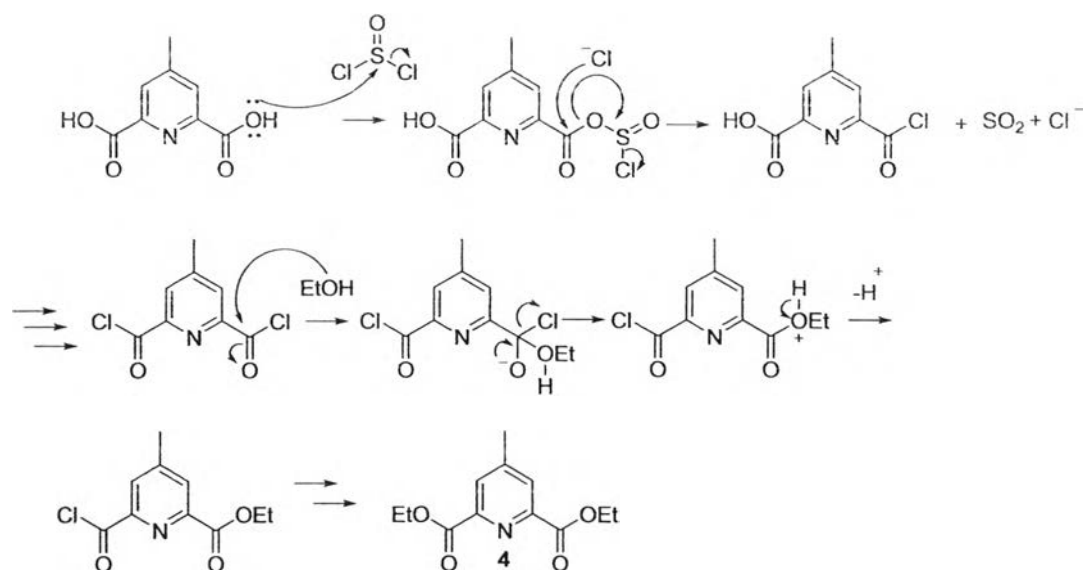
4.1.4 Diethyl 4-methylpyridine-2,6-dicarboxylate (4)

Compound 4 was synthesized by malonate condensation between compound 3 and a malonate salt followed by decarboxylation. Esterification of the resulting diacid gave compound 4 as a product [31]. Mechanism for synthesis compound 4 showed scheme 4.5.

The $^1\text{H-NMR}$ spectrum of compound 4 showed a singlet signal of the pyridine protons at 8.07 ppm (2H) and ethyl ester protons showed a quartet signal at 4.44 ppm (4H) coupled with a triplet signal at 1.42 ppm (6H) with a coupling constant of 7.2 Hz. These ester peaks slightly shifted to up field compared with compound 3 due to the disappearance of the chlorine atom (Figure A.7). Beside the methyl protons appeared a singlet signal at 2.48 ppm (3H) also confirmed the formation of compound 4.





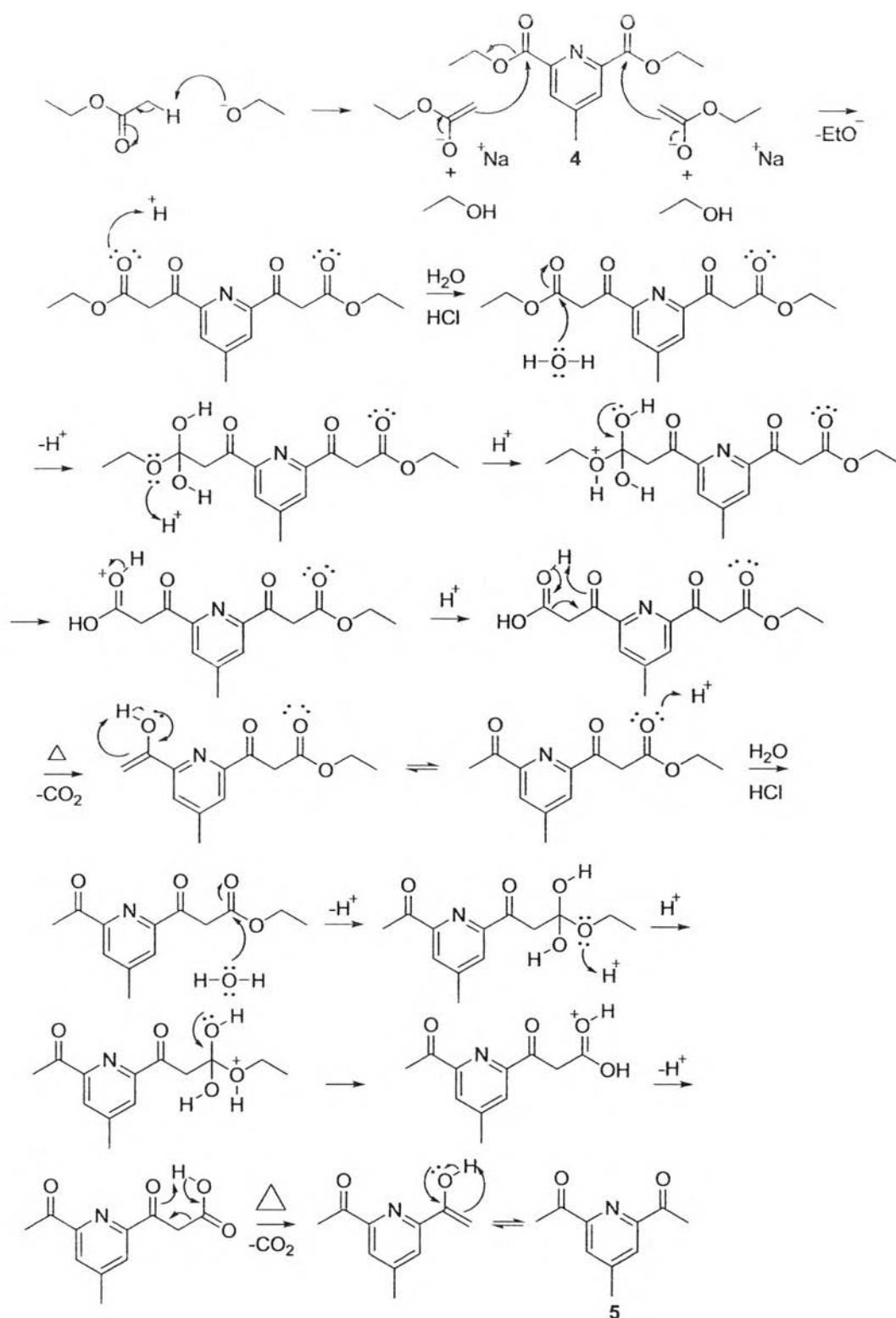


Scheme 4.5 Mechanism of the synthesis of compound 4

4.1.5 1,1'-(4-methylpyridine-2,6-diyl)diethanone (5)

Compound 5 was successfully synthesized by a modified procedure from a previous literature [32]. Claisen condensation between compound 4 and ethyl acetate using NaOEt as a base gave β keto ester thus was then hydrolysed to a β keto carboxylic acid. After decarboxylation the subsequent diketone was yielded as compound 5 in 17% yield. Mechanism for synthesis compound 5 is shown in Scheme 4.6





Scheme 4.6 Mechanism of the synthesis of compound 5

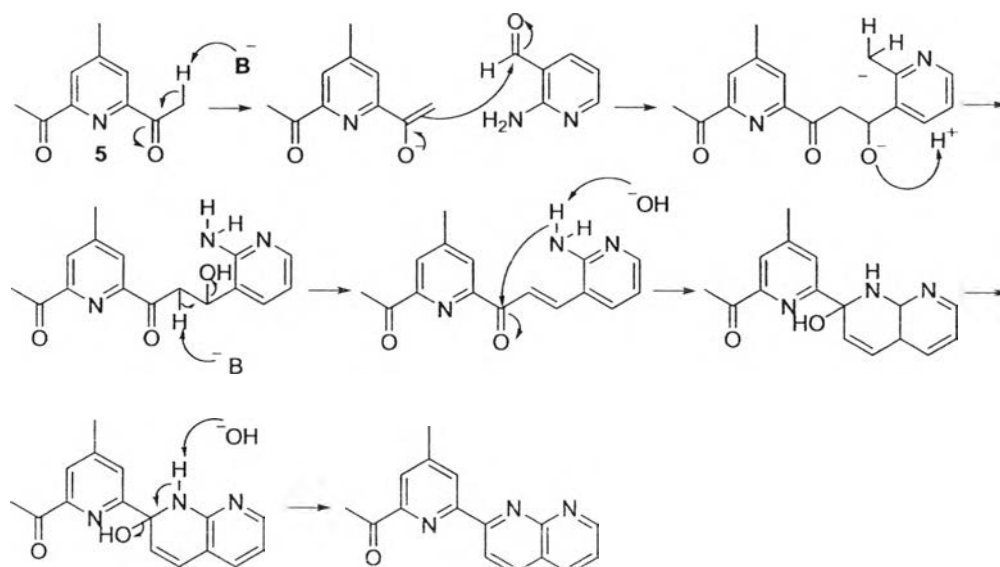


2815213942

The $^1\text{H-NMR}$ spectrum of compound **5** showed the disappearance of ethyl ester protons of compound **4** and showed a singlet signal of the pyridinyl protons at 8.03 ppm (2H) and the methyl protons at 2.49 ppm (3H) which were similar to the signals of the pyridinyl protons and the methyl protons of compound **4**. Besides compound **5** showed a singlet signal of the methyl ketone at 2.78 ppm (6H) (Figure A.8). From HR-ESI mass spectra, a molecule ion peak was observed at m/z 200.0691 ($[\text{M} + \text{Na}]^+$), compared to the calculation value at 200.0678 ($[\text{M} + \text{Na}]^+$) (Figure A.10), confirming the formation of compound **5**. The compound **5** can be dissolved in various common organic solvents such as CH_2Cl_2 , EtOAc, toluene, etc.

4.1.6 2,2'-(4-methylpyridine-2,6-diyl-bis-naphthyridine) (**6**)

Compound **6** was successfully synthesized by a modified procedure from a previous literature [34]. Friedlander condensation between compound **5** and 2-aminonicotinaldehyde gave compound **6** in 68% yield. Mechanism for the synthesis of compound **6** is shown in Scheme 4.7.



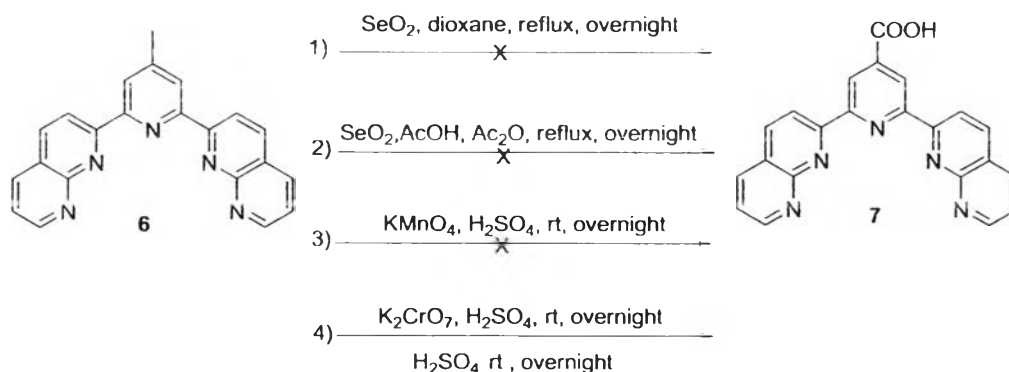
Scheme 4.7 Mechanism of the synthesis of compound **6**

From the $^1\text{H-NMR}$ spectrum of compound **6** (Figure A.11) showed singlet signals of methyl 2.65 ppm. Both acetyl groups compound **5** were converted to naphthyridine. Therefore the NMR signal of both acetyl groups at 2.78 ppm disappeared. Signal of proton position **g** appeared at 9.18 (2H) ppm as doublet of doublet with coupling constants 4.0 Hz and 1.6 Hz. The proton signal for position **c** and **d** appeared at 9.00 (2H) ppm and 8.38 (2H) as a consequence of their coupling, exhibited doublet separated with coupling constants 8.4 Hz. The proton signal for position **e** and **f** appeared at 8.27 (2H) ppm and 7.53 (2H) ppm as doublets of doublets, coupling between them and with proton position **g**, with coupling constants 1.6, 8.0 Hz. From ESI-HR mass spectra, a molecule ion peak was observed at m/z 372.1239 ($[\text{M} + \text{Na}]^+$), compared to the calculation value at 372.1225 ($[\text{M} + \text{Na}]^+$) (Figure A.15), confirming the formation of compound **6**. Solubility of compound **6** was scarcely soluble in common organic solvent. Compound **6** can be dissolved in CH_2Cl_2 and CHCl_3 .

4.1.7 2,6-Di(1,8-naphthyridine-2-yl)isonicotinic acid (**7**)

Compound **7** was synthesized by an oxidation of the methyl group in compound **6**. There are 4 possible synthesis pathways for compound **7** as shown in Scheme 4.8.





Scheme 4.8 Synthetic pathway of compound 7

Oxidation with selenium dioxide in dioxane [35], the first pathway, was not successful due to the poor solubility of compound 7 in the dioxane. Hence the compound 6 cannot react with selenium dioxide. Even though, the compound 6 dissolved well in acetic acid, oxidation with selenium dioxide in acetic acid was also failed. These suggested that selenium dioxide is too weak to oxidize compound 6. Consequently, a stronger oxidizing agent was required. In pathway 3 [36], potassium permanganate can successfully oxidize compound 6, but there was a complication in the work up process caused by the MnO_2 by product.

The oxidation process can be finally done using potassium dichromate [6] and compound 7 was collected as a green solid in 48% yield. A molecular ion peak was observed from MALDI-TOF spectra. This indicated the presence of compound 7 and its Cr complex, Thus demetallation was required.

The demetallation can be achieved by a procedure from a previous literature [33]. The product from oxidation was stirred in sulfuric acid for overnight, the compound 8 was obtained in 70% yield. The MALDI-TOF mass spectra of the product before, after demetallation and possible structures of the crude product were shown in Figure 4.1.

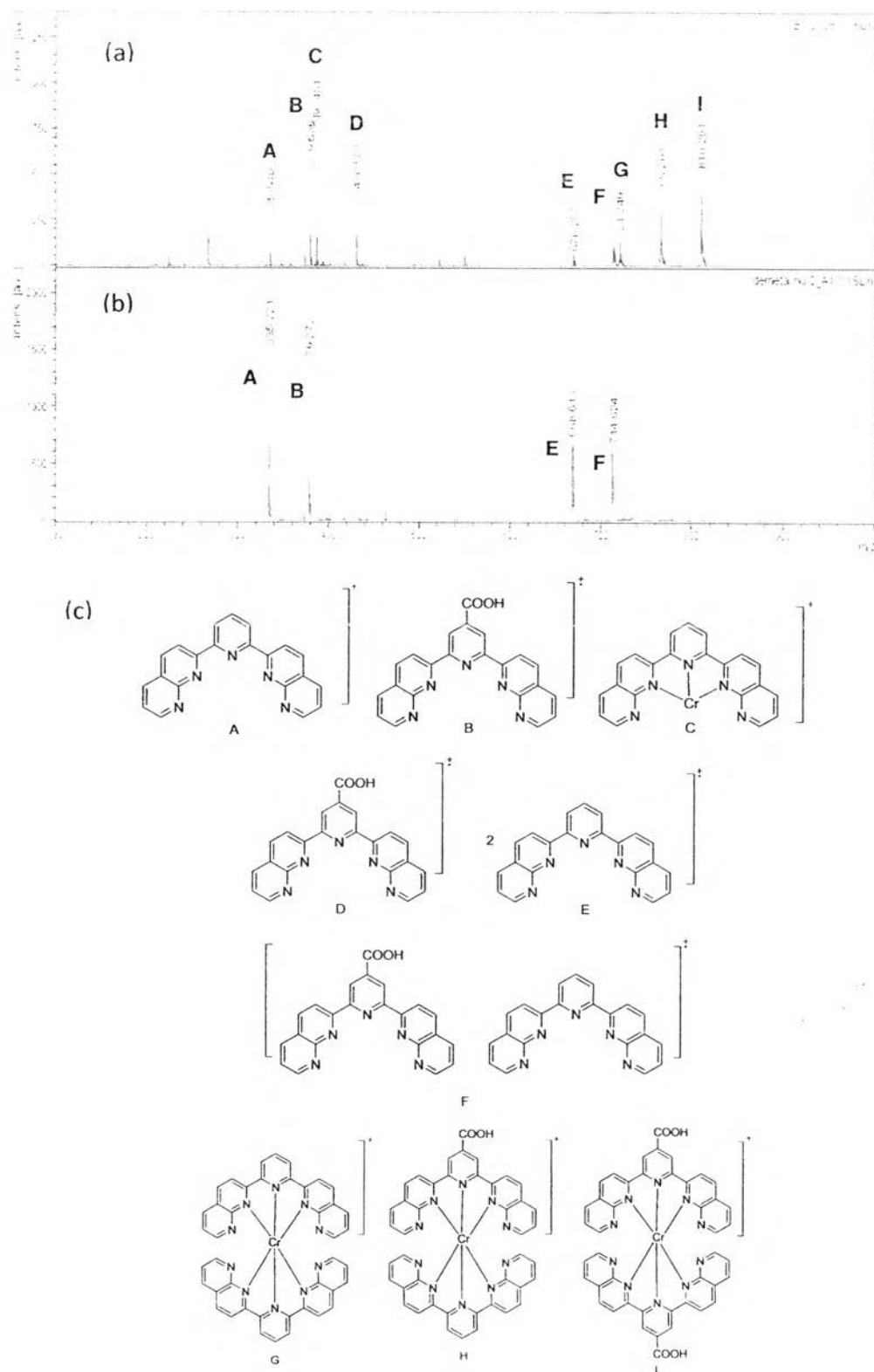


Figure 4.1 MALDI-TOF mass spectrum of the crude product (a) before and (b) after demetallation. (c) Possible structures of the crude product

After demetallation, a molecular ion peak of Cr complex at the position C, D, G, H and I disappeared indicating the success of demetallation. High resolution mass spectra (HR-ESI-MS) also showed a molecular ion peak at m/z 402.0971 ($[M+Na]^+$), confirming the formation of compound 7. The sulfuric acid was used in both oxidation and demetallation. In oxidation process, sulfuric acid converted the $K_2Cr_2O_7$ to H_2CrO_4 to oxidize the methyl group to carboxylic group. The Cr complex formed with nitrogen and excess dichromate. In demetallation process, nitrogen atom was protonated by sulfuric acid so Cr was washed away.

Though the 1H -NMR pattern of compound 7 was similar to that of compound 6 with the disappearance the proton of methyl group signal (position a). Also, the singlet peak the central pyridine ring (position b) shifted from 8.63 to 9.21 ppm caused by the electronic effect of carboxylic group. The proton signal of central pyridine ring overlapped with proton signal of position g and thus integration of this was equal to 2.09 (Figure 4.2).

IR spectrum of a solid sample of compound 7 showed the absorption of C=N stretching and C=C stretching at $1,602\text{ cm}^{-1}$ and $1,553\text{ cm}^{-1}$, respectively which similar to compound 6. But absorption of C=O stretching at $1,713.81\text{ cm}^{-1}$ and O-H stretching at $3,200\text{--}3,500\text{ cm}^{-1}$ in compound 7 was observed as the characteristic absorption of carboxylic group (Figure 4.3). Beside absorption of C-H stretching of methyl at $2,925\text{ cm}^{-1}$ was not observed in compound 7. Solubility of compound 7 was soluble in hot DMSO.



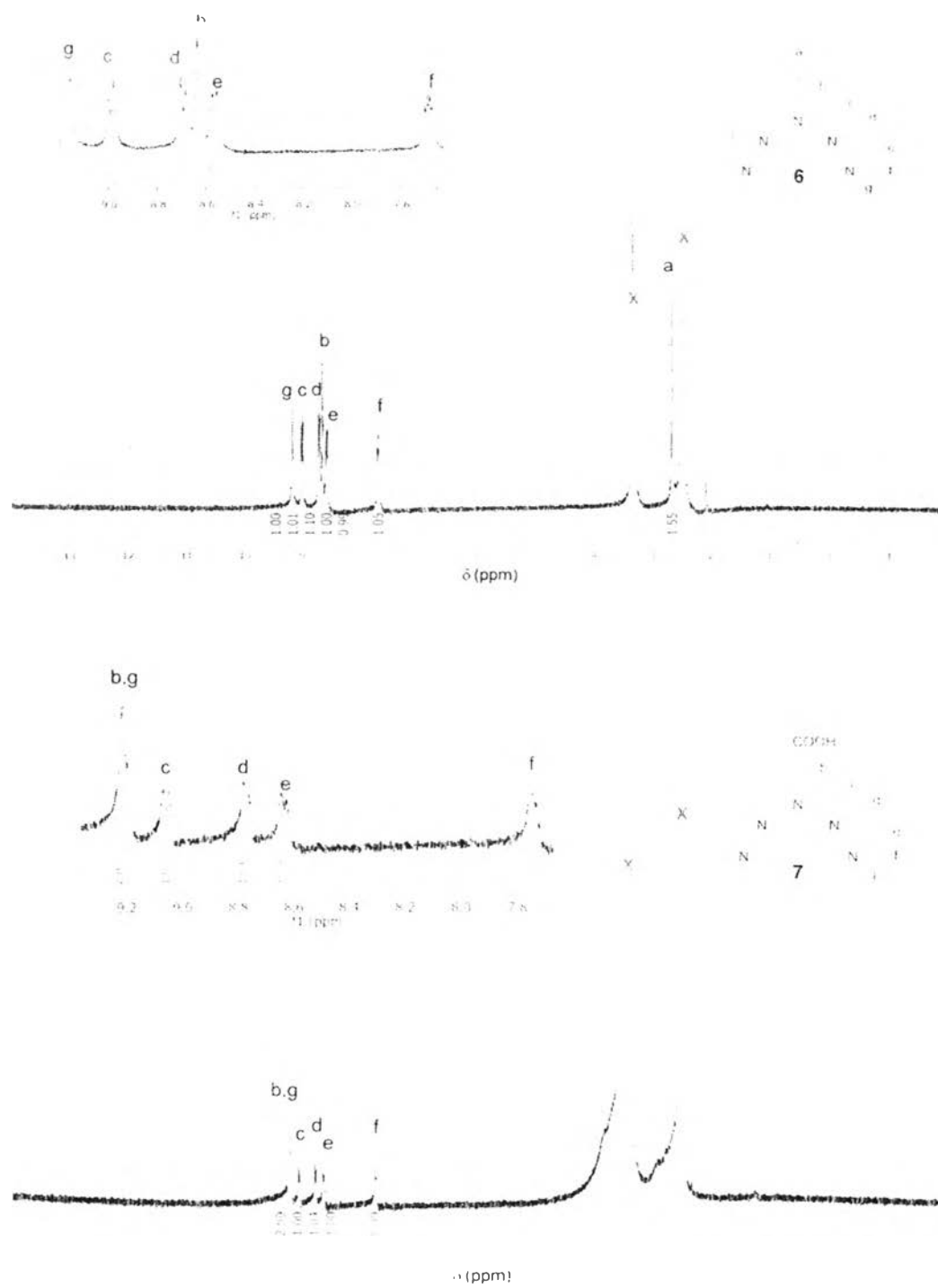


Figure 4.2 $^1\text{H-NMR}$ spectra of compounds 6 and 7

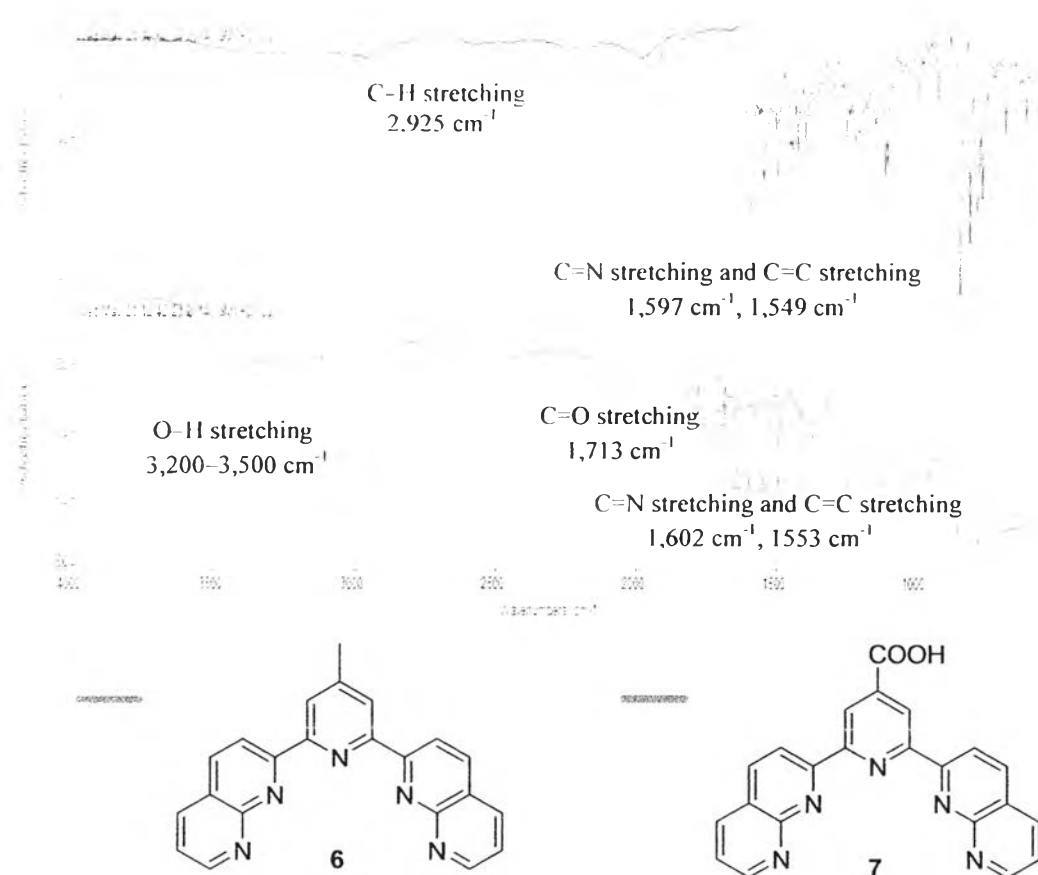


Figure 4.3 IR spectra of compounds 6 and 7

4.1.8 Ruthenium complex of 2,6-di(1,8-naphthylidene-2-yl)isonicotinic acid (8)

Compound 8 was synthesized by a modified procedure from previous literature [10] *via* refluxing of compound 7 with RuCl₃·nH₂O in ethanol. Compound 8 precipitated as dark green powder in 61% yield. The calculated exact mass of compound 8 was equal to 585.9178. The MALDI-TOF mass spectra on showed a molecular ion peak at m/z 436.391 ([M-CO₂-Cl₃]⁺) and 772.963 [2(M-CO₂-Cl₃)-Ru]⁺ as a dimer (Figure 4.4 (a)). Mass spectrum indicated the missing of carboxylic and chlorine atom caused by ionization process. High resolution mass spectrum on showed a molecular ion peak at m/z 549.94580 ([M-H-Cl]⁺) (Figure 4.4 (b)) and showed isotopic distributions peak as shown in Figure 4.5. Further observation of

these peaks showed isotopic distributions that were similar to the isotopic distributions from theoretical calculation as shown in Figure 4.5. The isotope distributions of these peaks were isotopic pattern of Ruthenium and molecular ion of COO. It indicated the presence of Ruthenium and carboxylic group in structure.

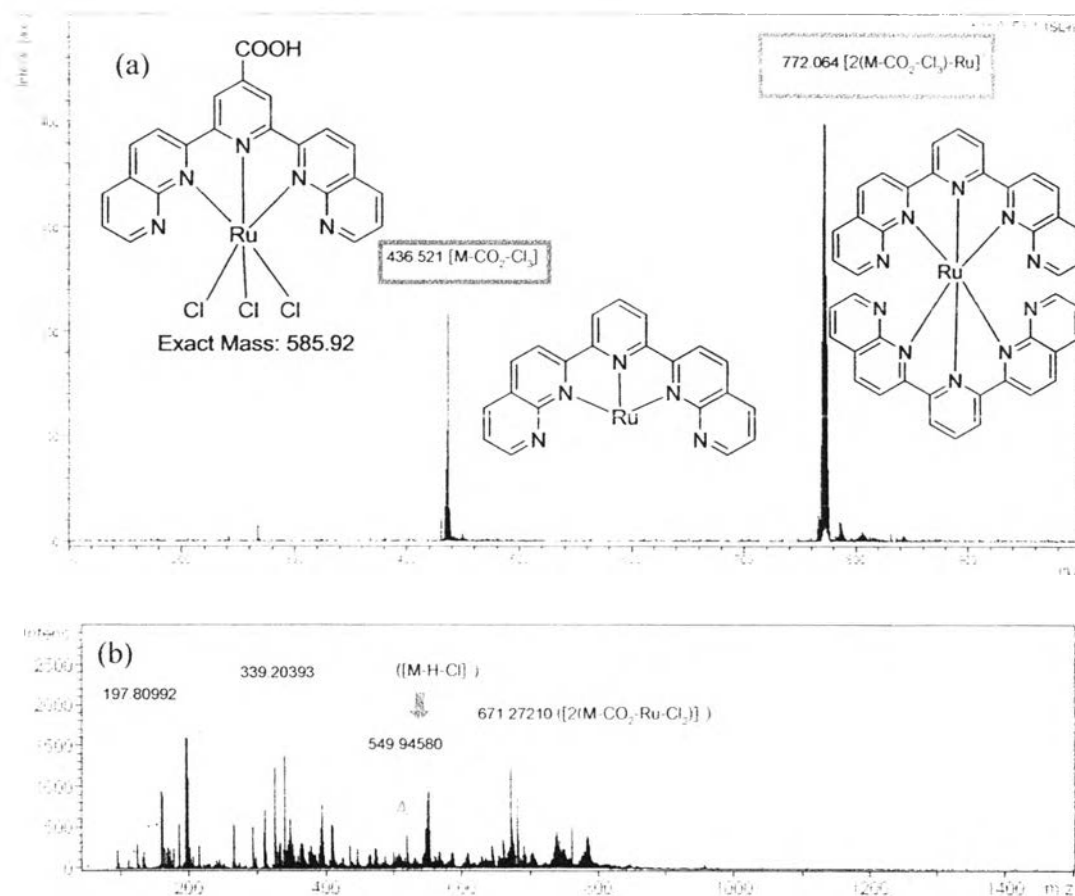
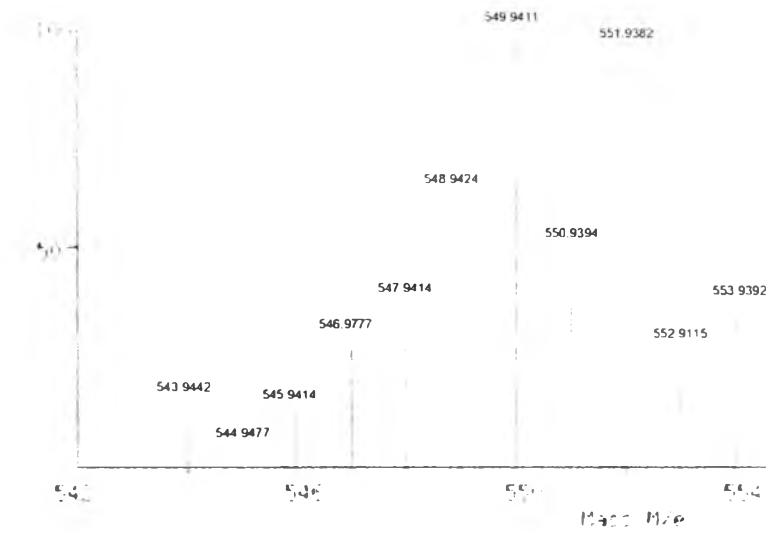


Figure 4.4 Mass spectra and structure compound 8 (a) MALDI-TOF MS and (b) HR-ESI MS

(a)



(b)



Figure 4.5 (a) calculated and (b) observed isotopic distributions of peak A

Furthermore, IR spectrum of a solid sample of compound **8** showed the absorption of C=O stretching and O–H stretching as the characteristic absorption of carboxylic group (Figure 4.6). Compound **7** was soluble in hot DMSO.

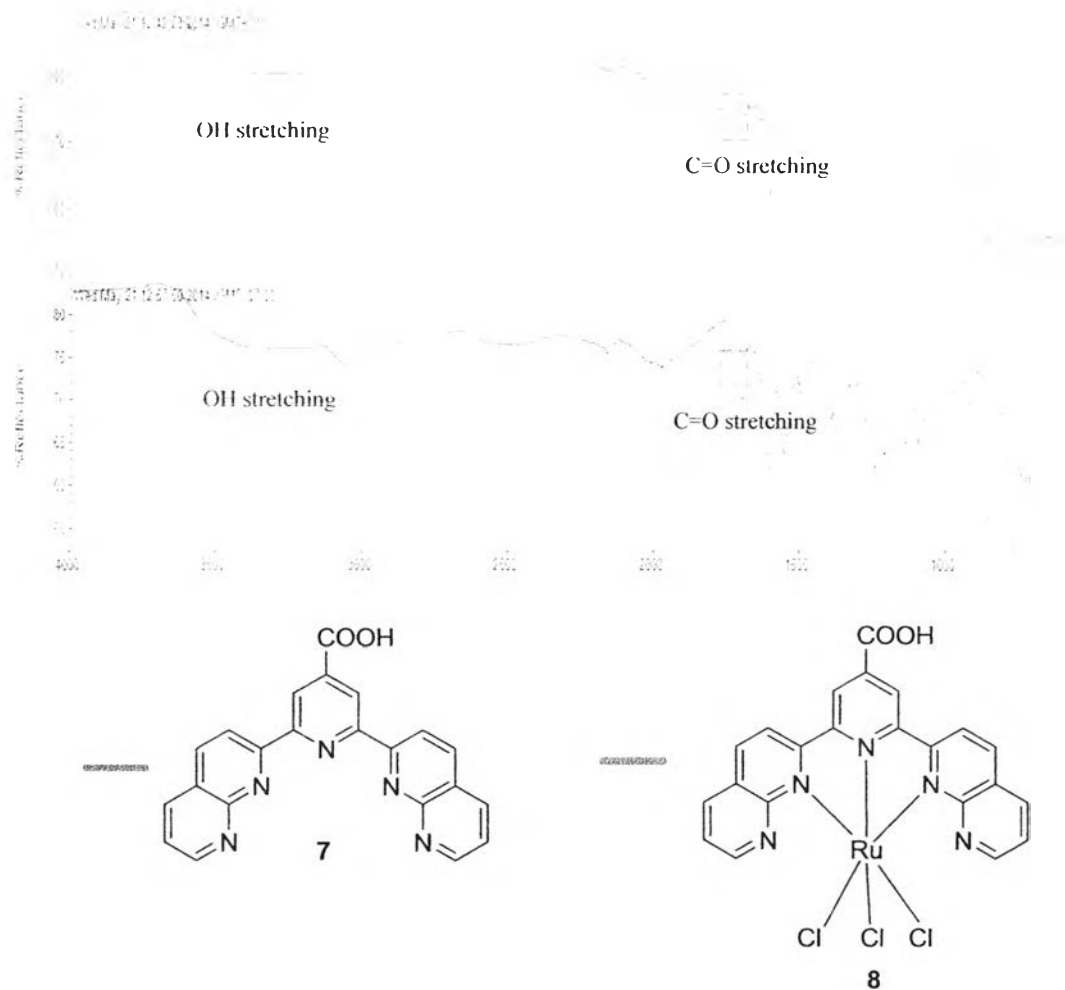


Figure 4.6 IR spectra of compound **7** and compound **8**

4.2 Investigation of photophysical properties

The physical properties of compound **6,7** and **8** were investigated by UV-Vis and Fluorescent spectrophotometry.

4.2.1 Absorption

UV-Vis spectra of compounds **6**, **7** and **8** were in DMSO and shown in Figure 4.7

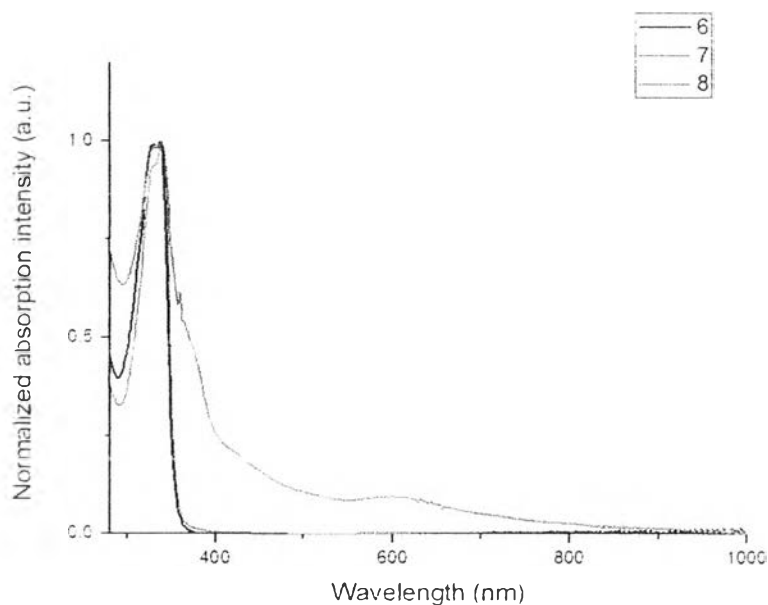


Figure 4.7 Normalized UV-Vis spectra of compounds **6** (black line), **7** (red line) and **8** (blue line)

UV-Vis spectra of compounds **6**, **7** and **8** showed strong absorption at the 300–400 nm with a similar characteristic absorption pattern as that of bis-naphthypyridine (bnp) as reported in previous literature [10, 11]. This absorption was resulted from π – π^* transition associated with the aromatic ring of the naphthyridine ligands. Compounds **6**, **7** and **8** showed absorption maxima at 337 nm, 340 nm and 340 nm, respectively. Moreover, compound **8** showed another absorption band at 400–800 nm. The intense bands in the visible region observed in compound **8**. This was caused metal to ligand charge transfer (MLCT) from π orbital of Ru to π^* orbital of the ligand [10, 11].

4.2.2 Emission

The emission spectra of compounds **6**, **7** and **8** were recorded in DMSO and are shown in Figure 4.8

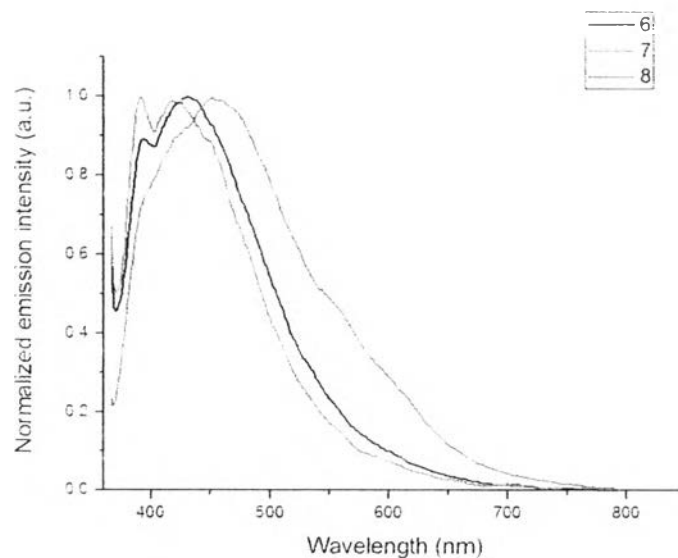


Figure 4.8 Emission spectra of compounds **6** (black line), **7** (red line) and **8** (blue line)

Upon excitation at 350 nm, compounds **6**, **7** and **8** showed similar emission pattern with low intensity at 440, 435 and 465 nm, respectively. The emission maximum of compound **8** leads to red shift emission because of the lowered energy gap between the π orbital of Ru to π^* orbital of the ligands [37].